 CMES, vol.45, no.3, pp.227-247, 2009

Boundary Layer Effect in BEM with High Order Geometry Elements Using Transformation

Y.M. Zhang[1], Y. Gu[1] and J.T. Chen[2]

Abstract: The accurate evaluation of nearly singular integrals is one of the major concerned problems in the boundary element method (BEM). Although the current methods have achieved great progress, it is often possible only for problems defined in the simplest geometrical domains when the nearly singular integrals need to be calculated. However, engineering processes occur mostly in complex geometrical domains, and always, involve nonlinearities of the unknown variables and its derivatives. Therefore, effective methods of dealing with nearly singular integrals for such practical problems are necessary and need to be further investigated. In this paper, a general strategy based on a nonlinear transformation is introduced and applied to evaluate the nearly singular integrals in two dimensional (2D) elasticity problems. The proposed nonlinear transformation method can figure out the rapid variations of nearly singular kernels and extremely high accuracy of numerical results can be achieved without increasing other computational efforts. The accuracy and efficiency of the method are demonstrated through three examples that are commonly encountered in the applications of the BEM.

Keywords: BEM, nearly singular integrals, transformation, high-order elements, elasticity problem.

1 Introduction

Accurate and efficient evaluation of singular and nearly singular integrals is an important issue in boundary element analysis. These integrands are singular functions when the collocation point belongs to the integration elements, and many effective methods [Atluri (2004), (2005); Atluri, Liu and Han (2006); Brebbia *et al.* (1984); Chen (2002, 2000); Davies *et al.* (2007);Li, Wu and Yu (2009); Sanz

[1] Institute of Applied Mathematics, Shandong University of Technology, Zibo 255049, P.R. China. Email: zymfc@163.com

[2] Department of Harbor and River Engineering, National Taiwan Ocean University, Keelung 20224, Taiwan. Email: jtchen@mail.ntou.edu.tw

et al. (2007);Sun (1999); Tanaka, Sladek (1994); Guiggiani (1992); Gray *et al.* (2006); Young *et al.* (2007); Zhang and Wen (2004)] have been developed to deal with them. If the collocation point is close to but not on the integration elements, the ensuring integrals are termed nearly weak singular, nearly strong singular and nearly hyper-singular integrals, which are not singular in the sense of mathematics. However, from the point of view of numerical integrations, these integrals can not be calculated accurately by using the standard Gaussian quadrature. This is so-called boundary layer effect in BEM.

The accurate evaluation of nearly singular integrals plays an important role in many engineering problems. In general, these include evaluating the solution near the boundary in potential problems and calculating displacements and stresses near the boundary in elasticity problems, for example, contact problems, displacement around crack tips, sensitivity problems and thin-body problems [Chen and Liu (2001); Albuquerque and Aliabadi (2008); Guz *et al.* (2007); Karlis *et al.* (2008)].

Owing to the importance of the nearly singular integrals, a great amount of attention has been attracted and many numerical methods and techniques have been developed in recent years. The proposed methods include, but are not limited to, virtual boundary element method [Sun (1999); Zhang and Sun (2000)], rigid-body displacement method or the simple solution method [Chen *et al.* (1998); Cruse (1974); Lachat and Watson (1976); Liu *et al.* (2008); Wang *et al.* (1994); Mukerjee (2000); Sladek and Tanaka (1993); Granados and Gallego (2001)], interval subdivision method [Jun (1985); Tanaka (1991); Gao (2008)], special Gaussian quadrature method [Earlin (1992); Lifeng (2004)], analytical or semi-analytical methods [Yoon and Heister (2000); Zhang and Sun (2001); Friedrich (2002); Fratantonio and Rencis (2000); Zhang and Zhang (2004); Cruse and Aithal (1993); Schulz (1998); Liu (1998); Zhou et al. (2008); Niu (2007)]. In a recent study, the above methods have been reviewed in detail by Zhang et al. [Zhang and Sun (2008)].

At present, the most common methods for calculating nearly singular integrals are various nonlinear transformations, for example, the cubic polynomial transformation [Telles (1987)], the bi-cubic transformation [Cerrolaza and Alarcon (1989)], the sigmoidal transformation [Johnston (1999)], the semi-sigmoidal transformation [Johnston (2000)], the coordinate optimization transformation [Sladek, Sladek and Tanaka (2000)], the attenuation mapping method [Earlin (1993); Luo et al. (1998)], the rational transformation [Huang and Cruse (1993)], and the distance transformation [Ma and Kamiya (2002)]. The basic ideas of the above transformations can be generalized into two categories: one is removing the nearly zero factor by using another zero factor which usually generated by Jacobian; the other one is converting the nearly zero factor in the denominator to be part of the numerator, which profits from the idea of the reciprocal transformation for the regularization

of weakly singular integrals. Numerical tests show that the transformations based on the former idea are effective for the calculation of weakly singular integrals but not satisfactory for strong singular or hypersingular integrals. The latter transformations, based on the idea of reciprocal transformation, can convert nearly singular kernels into regular kernels, but the original regular parts behave nearly singular after the transformations, so they are suitable only for a case when the regular part of the integrand is constant.

For most of current numerical methods, the geometry of the boundary element is often depicted by using linear shape functions when nearly singular integrals need to be calculated. However, most engineering processes occur mostly in complex geometrical domains, and obviously, higher order geometry elements are expected to be more accurate [Atluri (2005)]. To improve the calculation accuracy and efficiency of the nearly singular integrals, efficient approaches for estimating nearly singular integrals over high-order geometry elements are necessary and need to be further investigated.

When the geometry of the boundary element is approximated by using high order elements—usually of second order, the Jacobian $J(\xi)$ is not a constant but a non-rational function which can be expressed as $\sqrt{a+b\xi+c\xi^2}$, where a,b and c are constants, ξ is the dimensionless coordinate; The distance r between the field points and the source point is a non-rational function of the type $\sqrt{p_4(\xi)}$, where $p_4(\xi)$ is the fourth order polynomial. Thus, the forms of the integrands in boundary integrals become more complex, and it is, generally, more difficult to implement when nearly singular integrals need to be calculated.

This paper aims to develop a general strategy suitable for calculating the nearly singular integrals occurring on high order geometry elements. A general nonlinear transformation technique [Zhang and Sun (2008)] is adopted to remove the near singularities of kernels' integration by smoothing out the rapid variations of the integrand of nearly singular integrals. The strategy proposed in this paper adopted isoparametric quadratic elements to describe the integral kernel functions and the Jacobean. Owing to the employment of the parabolic arc, only a small number of elements need to be divided along the boundary, and high accuracy can be achieved without increasing more computational efforts. In addition, the non-singular BIEs of indirect variables [Zhang and Wen (2004)] were employed to estimate the singular integrals occurring on curved boundaries. Three numerical examples of elastic problems are given, with results, showing the high efficiency and the stability of the suggested approach, even when the internal point is very close to the boundary.

2 Non-singular boundary integral equations (BIEs)

It is well known that the domain variables can be computed by integral equations only after all the boundary quantities have been obtained, and the accuracy of boundary quantities directly affects the validity of the interior quantities. However, when calculating the boundary quantities, we have to deal with the singular boundary integrals, and a good choice is using the regularized BIEs. Therefore, for avoiding the "boundary layer effect", two aspects are necessary. One is the accurate computation of the boundary functions, which is generally carried out by adopting the regularized BIEs; the other is an efficient algorithm of calculating the nearly singular integrals.

In this paper, we always assume that Ω is a bounded domain in R^2, Ω^c is its open complement, and Γ denotes the boundary. $\mathbf{t}(\mathbf{x})$ and $\mathbf{n}(\mathbf{x})$ (or $\mathbf{t}$ and $\mathbf{n}$) are the unit tangent and outward normal vectors of Γ to the domain Ω at the point $\mathbf{x}$, respectively. For 2D elastic problems, the non-singular BIEs with indirect variables are given in [Zhang and Wen (2004)]. Without regard to the rigid body displacement and the body forces, the non-singular BIEs on Ω^c can be expressed as

$$u_i(\mathbf{y}) = \int_\Gamma \varphi_k(\mathbf{x}) u_{ik}^*(\mathbf{y},\mathbf{x}) d\Gamma, \mathbf{y} \in \Gamma \tag{1}$$

$$\begin{aligned}\nabla u_i(\mathbf{y}) = &\int_\Gamma [\varphi_k(\mathbf{x}) - \varphi_k(\mathbf{y})] \nabla u_{ik}^*(\mathbf{y},\mathbf{x}) d\Gamma - \varphi_k(\mathbf{y}) \left\{ \int_\Gamma [\mathbf{t}(\mathbf{x}) - \mathbf{t}(\mathbf{y})] \frac{\partial u_{ik}^*(\mathbf{y},\mathbf{x})}{\partial \mathbf{t}} d\Gamma \right. \\ &+ \int_\Gamma [\mathbf{n}(\mathbf{x}) - \mathbf{n}(\mathbf{y})] \frac{\partial u_{ik}^*(\mathbf{y},\mathbf{x})}{\partial \mathbf{n}} d\Gamma + \frac{k_0}{G} \mathbf{n}(\mathbf{y}) \left(\int_\Gamma [n_k(\mathbf{x}) - n_k(\mathbf{y})] \frac{\partial \ln r}{\partial x_i} d\Gamma \right. \\ &\left. \left. + n_k(\mathbf{y}) \int_\Gamma [t_i(\mathbf{x}) - t_i(\mathbf{y})] \frac{\partial \ln r}{\partial \mathbf{t}} d\Gamma + n_k(\mathbf{y}) \int_\Gamma [n_i(\mathbf{x}) - n_i(\mathbf{y})] \frac{\partial \ln r}{\partial \mathbf{n}} d\Gamma \right) \right\}, \\ &\mathbf{y} \in \Gamma\end{aligned} \tag{2}$$

For the domain Ω, the nonsingular BIEs are given as

$$u_i(\mathbf{y}) = \int_\Gamma \varphi_k(\mathbf{x}) u_{ik}^*(\mathbf{x},\mathbf{y}) d\Gamma, \mathbf{y} \in \Gamma \tag{3}$$

$$\begin{aligned}\nabla u_i(\mathbf{y}) =& \varphi_k(\mathbf{y})\mathbf{n}(\mathbf{y})\frac{1}{G}[\delta_{ik}-\frac{n_k(\mathbf{y})n_i(\mathbf{y})}{2(1-\nu)}]+\int_\Gamma[\varphi_k(\mathbf{x})-\varphi_k(\mathbf{y})]\nabla u^*_{ik}(\mathbf{y},\mathbf{x})d\Gamma\\ &-\varphi_k(\mathbf{y})\left\{\int_\Gamma[\mathbf{t}(\mathbf{x})-\mathbf{t}(\mathbf{y})]\frac{\partial u^*_{ik}(\mathbf{y},\mathbf{x})}{\partial \mathbf{t}}d\Gamma+\int_\Gamma[\mathbf{n}(\mathbf{x})-\mathbf{n}(\mathbf{y})]\frac{\partial u^*_{ik}(\mathbf{y},\mathbf{x})}{\partial \mathbf{n}}d\Gamma\right.\\ &+\frac{k_0}{G}\mathbf{n}(\mathbf{y})\left(\int_\Gamma[n_k(\mathbf{x})-n_k(\mathbf{y})]\frac{\partial \ln r}{\partial x_i}d\Gamma+n_k(\mathbf{y})\int_\Gamma[t_i(\mathbf{x})-t_i(\mathbf{y})]\frac{\partial \ln r}{\partial \mathbf{t}}d\Gamma\right.\\ &\left.\left.+n_k(\mathbf{y})\int_\Gamma[n_i(\mathbf{x})-n_i(\mathbf{y})]\frac{\partial \ln r}{\partial \mathbf{n}}d\Gamma\right)\right\},\\ &\mathbf{y}\in\Gamma\end{aligned} \tag{4}$$

For the internal point $\mathbf{y}$, the integral equations can be written as

$$u_i(\mathbf{y})=\int_\Gamma \varphi_k(\mathbf{x})u^*_{ik}(\mathbf{y},\mathbf{x})d\Gamma\ ,\ \mathbf{y}\in\hat{\Omega} \tag{5}$$

$$\nabla u_i(\mathbf{y})=\int_\Gamma \phi_k(\mathbf{x})\nabla u^*_{ik}(\mathbf{y},\mathbf{x})d\Gamma\ ,\ \mathbf{y}\in\hat{\Omega} \tag{6}$$

In Eqs. (1)–(6), $i,k=1,2$; $k_0=1/4\pi(1-\nu)$; G is the shear modulus; $\phi_k(\mathbf{x})$ is the density function to be determined; $u^*_{ik}(\mathbf{y},\mathbf{x})$ denotes the Kelvin fundamental solution. In Eqs. (5) and (6) $\hat{\Omega}=\Omega$ or Ω^c.

When the field point $\mathbf{y}$ is far from the boundary element, a straightforward application of Gaussian quadrature suffices to evaluate such integrals. However, when the field point $\mathbf{y}$ is very close to the integral element Γ_e, the distance r between the field point $\mathbf{y}$ and the source point $\mathbf{x}$ tends to zero. Thus, there exist nearly singular integrals in Eqs. (5) and (6). These nearly singular integrals can be expressed as

$$\begin{cases} I_1=\int_{\Gamma_e}\psi(\mathbf{x})\ln r^2 d\Gamma \\ I_2=\int_{\Gamma_e}\psi(\mathbf{x})\frac{1}{r^{2\alpha}}d\Gamma \end{cases} \tag{7}$$

where $\alpha>0$, $\psi(\mathbf{x})$ denotes a well-behaved function.

3 Nearly singular integrals under curvilinear elements

The quintessence of the BEM is to discretize the boundary into a finite number of segments, not necessarily equal, which are called boundary elements. Two approximations are made over each of these elements. One is about the geometry of the boundary, while the other has to do with the variation of the unknown boundary quantity over the element. The linear element is not an ideal one as it can not approximate with sufficient accuracy for the geometry of curvilinear boundaries.

For this reason, it is recommended to use higher order elements, namely, elements that approximate geometry and boundary quantities by higher order interpolation polynomials—usually of second order. In this paper, the geometry segment is modeled by a continuous parabolic element, which has three knots, two of which are placed at the extreme ends and the third somewhere in-between, usually at the midpoint. Therefore the boundary geometry is approximated by a continuous piecewise parabolic curve. On the other hand, the distribution of the boundary quantity on each of these elements is depicted by a discontinuous quadratic element, three nodes of which are located away from the endpoints.

Assume $\mathbf{x}^1 = (x_1^1, x_2^1)$ and $\mathbf{x}^2 = (x_1^2, x_2^2)$ are the two extreme points of the segment Γ_j, and $\mathbf{x}^3 = (x_1^3, x_2^3)$ is in-between one. Then the element Γ_j can be expressed as follows

$$x_k(\xi) = N_1(\xi)x_k^1 + N_2(\xi)x_k^2 + N_3(\xi)x_k^3, k = 1,2$$

where $N_1(\xi) = \xi(\xi-1)/2$, $N_2(\xi) = \xi(\xi+1)/2$, $N_3(\xi) = (1-\xi)(1+\xi)$, $-1 \leq \xi \leq 1$. As shown in Fig. 1, the minimum distance d from the field point $\mathbf{y} = (y_1, y_2)$

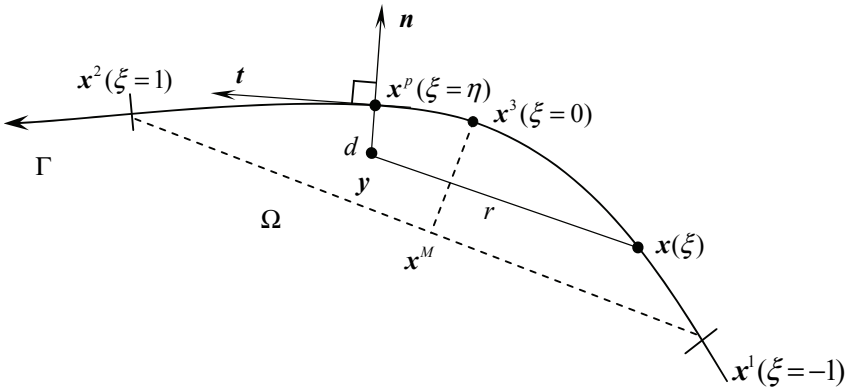

Figure 1: The minimum distance d from the field point y to the boundary element

to the boundary element Γ_j is defined as the length of $\overline{\mathbf{yx}^p}$, which is perpendicular to the tangential line $\mathbf{t}$ and through the projection point $\mathbf{x}^p$. Letting $\eta \in (-1,1)$ is the local coordinate of the projection point$\mathbf{x}^p$, i.e. $\mathbf{x}^p = (x_1(\eta), x_2(\eta))$. Then η is the real root of the following equation

$$x_k'(\eta)(x_k(\eta) - y_k) = 0 \tag{8}$$

If the field point **y** sufficiently approaches the boundary, then Eq. (8) has a unique real root. In fact, setting

$$F(\eta) = x_k'(\eta)(x_k(\eta) - y_k)$$

there is

$$F'(\eta) = x_k'(\eta)x_k'(\eta) + x_k''(\eta)(x_k(\eta) - y_k) = J^2(\eta) + x_k''(\eta)(x_k(\eta) - y_k)$$

where $J(\eta)$ is the Jacobian of the transformation from parabolic element to the line interval $[-1,\ 1]$. Therefore, when the field point **y** is sufficiently close to the element, we explicitly have $F'(\eta) > 0$.

The unique real root of Eq. (8) can be evaluated numerically by using the Newton's method or computed exactly by adopting the algebraic root formulas of 3-th algebraic equations. In this paper, two ways are all tested, and practical applications show that both ways can be used to obtain desired results. Furthermore, the Newton's method is more simple and effective, especially if the initial approximation is properly chosen and if we can do this, only two or three iterations are sufficient to approximate the real root. For the root formula of 3-th algebraic equations, let's consider the following algebraic equation

$$ax^3 + bx^2 + cx + d = 0$$

if there exists only one real root, the analytical solution can be expressed as follows

$$x = -\frac{b}{3a} + \frac{2(\sqrt{s^2+t^2})^{\frac{1}{3}}}{3\sqrt[3]{2a}} \cos\left(\frac{1}{3}\arccos\frac{s}{\sqrt{s^2+t^2}}\right)$$

where $s = -2b^3 + 9acb - 27a^2d$, $t = \sqrt{-4(3ac-b^2)^3 - (-2b^3+9acb-27a^2d)^2}$.

Using the procedures described above, we can obtain the value of the real root η. Thus, we have

$$\begin{aligned} x_k - y_k =& x_k - x_k^p + x_k^p - y_k \\ =& \frac{1}{2}(\xi - \eta)\left[(x_k^1 - 2x_k^3 + x_k^2)(\xi + \eta) + (x_k^2 - x_k^1)\right] + x_k(\eta) - y_k \end{aligned} \tag{9}$$

By using Eq. (9), the distance square r^2 between the field point **y** and the source point $\mathbf{x}(\xi)$ can be written as

$$r^2(\xi) = (x_k - y_k)(x_k - y_k) = (\xi - \eta)^2 g(\xi) + d^2 \tag{10}$$

where $d^2 = (x_k(\eta) - y_k)(x_k(\eta) - y_k)$,

$$\begin{aligned} g(\xi) =& \frac{1}{4}(x_k^1 - 2x_k^3 + x_k^2)(x_k^1 - 2x_k^3 + x_k^2)(\xi + \eta)^2 \\ &+ \frac{1}{2}(x_k^1 - 2x_k^3 + x_k^2)(x_k^2 - x_k^1)(\xi + \eta) \\ &+ h^2 + (x_k^1 - 2x_k^3 + x_k^2)\,(x_k(\eta) - y_k), \end{aligned}$$

where $h = \frac{1}{2}\sqrt{(x_k^2 - x_k^1)(x_k^2 - x_k^1)}$.

Apparently, there is $g(\xi) \geq 0$.

By some simple deductions, the nearly singular integrals in Eq. (7) would be reduced to the following two types

$$\mathrm{I} = \int_0^A f(\xi) \ln\left(\xi^2 g(\xi) + d^2\right) d\xi \tag{11}$$

$$\mathrm{II} = \int_0^A \frac{f(\xi)}{(\xi^2 g(\xi) + d^2)^\alpha} d\xi \tag{12}$$

where A is a constant which is possibly with different values in different element integrals; $f(\cdot)$ is a regular function that consists of shape function, Jacobian and ones which arise from taking the derivative of the integral kernels.

4 Variable transformation

The main reason why nearly singular integrals can not be calculated accurately by using the standard Gaussian quadrature, in common observation, is caused by some bad qualities of the nearly singular kernels such as the fiercer oscillation and the unboundedness of the integrands. However, in the authors' opinion, that is not true. Some regular integral kernels, such as $\frac{x^2}{x^2+c^2}$ or $\frac{x^4}{x^2+c^2}$ which are obviously neither unbounded nor oscillating rapidly during the integral interval, still can not be calculated accurately by using the standard Gaussian quadrature (See Figs. 2 and 3). For this phenomenon, we can also speculate that some methods such as attenuation mapping method, which eliminate the nearly zero factors by adopting another zero factors in the density function, would be not very effective, and the practices proved it. According to the authors' point of view, the main reason of this phenomenon is caused by the different orders of magnitude of the zero-divisor. In this section, a general variable transformation for high order boundary elements was constructed in order to diminish the difference of the orders of magnitude or the scale of change for operational factors. The constructed transformation can remove the near singularity efficiently and high accurate results can be obtained by using the standard Gaussian quadrature.

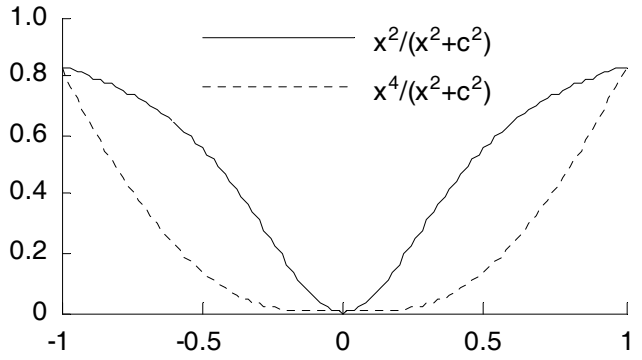

Figure 2: The images of two integral kernels with $c^2 = 0.2$

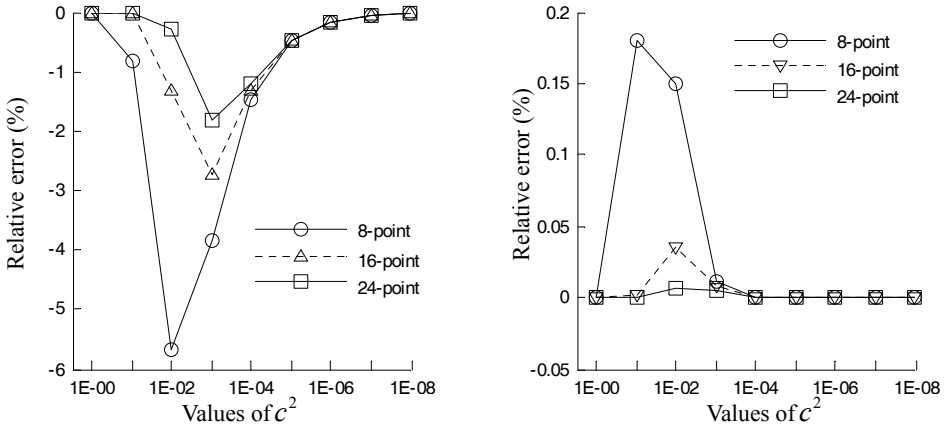

Figure 3: Relative errors of the computation results of $x^2/(x^2+c^2)$ and $x^4/(x^2+c^2)$ using 8-point/16-point/24-point Gaussian quadrature

Based on the idea of diminishing the difference of the orders of magnitude or the scale of changes of operational factors, we introduce the following transformation

$$\xi = d(e^{k(1+t)} - 1) \tag{13}$$

where $k = \frac{1}{2}\ln(1+\frac{A}{d})$.

Substituting (13) into Eqs. (11) and (12), then we obtain the following equations

$$\begin{aligned} \mathrm{I} =& 2kd\ln d\int_{-1}^{1} f(d(e^{k(1+t)}-1))e^{k(1+t)}dt \\ &+ kd\int_{-1}^{1} f(\xi)\ln\left((e^{k(1+t)}-1)^2 g(\xi)+1\right)e^{k(1+t)}dt \end{aligned} \tag{14}$$

$$\mathrm{II} = \frac{1}{d^{2\alpha-1}}\int_{-1}^{1} \frac{f(\xi)}{\left((e^{k(1+t)}-1)^2 g(\xi)+1\right)^{\alpha}} e^{k(1+t)}dt \tag{15}$$

where $\xi = d(e^{k(1+t)}-1)$.

By following the procedures described above, the near singularity of the boundary integrals has been fully regularized. The final integral formulations over parabolic elements are obtained as shown in Eqs. (14) and (15), which can be computed straightforward by using standard Gaussian quadrature.

5 Numerical examples

In this section, three examples of 2D elastostatics with curved boundaries are given to test the proposed method. Isoparametric quadratic elements are employed to approximate the geometrical elements and the boundary densities. The proposed transformation technique is used to estimate the nearly singular integrals when the interior points are very close to the integral elements.

Example 1 As shown in Fig. 4, a thick cylinder subjected to the uniform radial pressures $p = 5$ along the surfaces is considered. The inner and outer radii of the cylinder are 1 and 2, respectively. In this example, the elastic shear modulus is $G = 807692.3N/cm^2$, and the Poisson's ratio is $v = 0.3$.

Fifteen and ten quadratic elements are divided along the outer and inner surfaces, respectively. Therefore, the total number of the elements is 25.

The numerical solutions of the tangential stresses σ_θ at the interior points close to the outer and inner surfaces are listed in Tab. 1 and Tab. 2. Results of the radial stresses σ_r at the interior points close to the outer and inner surfaces are listed in Fig. 5 and Fig. 6, respectively. Both the CBEM and the proposed method are employed for the purpose of comparison. The convergence rates of the computed σ_θ at interior points $(1.0000001, 0)$ and $(1.9999999, 0)$ are shown in Fig.7.

It can be seen from Tab. 1 and Tab. 2 that the results of stresses σ_θ can be accurately calculated by using the CBEM and the present method when the computed points are not very close to the boundary ($r < 1.95$ or $r > 1.04$). However, when the distance between the interior point and the boundary is equal to or less than 0.04, the results calculated by the CBEM become less satisfactory or even invalid. In

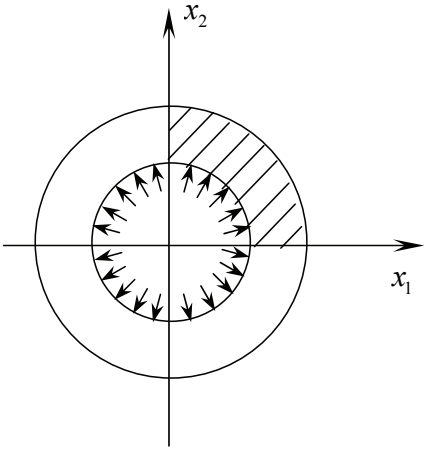

Figure 4: Thick cylinder subjected to the uniform radial pressure on the inner surface

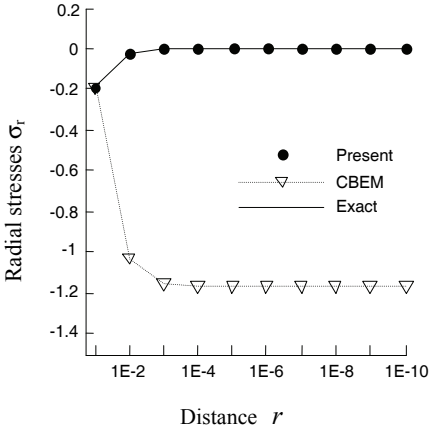

Figure 5: Radial stresses σ_r at interior points close to the outer surface

contrast with the CBEM, the present method can be used to obtain accurate results with the largest percentage error less than 0.1% even when the distance between the interior point and the outer boundary reaches10^{-10}.

Table 1: Tangential stresses σ_θ at interior points close to the outer surface

Radius r	Exact	CBEM	Present	Relative error
1.9	0.3513389E+01	0.3517443E+01	0.3513383E+01	0.1593349E-03
1.95	0.3419899E+01	0.3520995E+01	0.3418865E+01	0.3023558E-01
1.99	0.3350126E+01	0.3324564E+01	0.3347962E+01	0.6459433E-01
1.999	0.3335001E+01	0.2885692E+01	0.3332540E+01	0.7380650E-01
1.999 9	0.3333500E+01	0.2836292E+01	0.3331008E+01	0.7475973E-01
1.999 99	0.3333350E+01	0.2831348E+01	0.3330852E+01	0.7493745E-01
1.999 999	0.3333335E+01	0.2830854E+01	0.3330847E+01	0.7464263E-01
1.999 999 9	0.3333334E+01	0.2830804E+01	0.3330859E+01	0.7423208E-01
1.999 999 99	0.3333333E+01	0.2830799E+01	0.3330729E+01	0.7813735E-01
1.999 999 999	0.3333333E+01	0.2830799E+01	0.3330762E+01	0.7714073E-01
1.999 999 9999	0.3333333E+01	0.2830799E+01	0.3331151E+01	0.6546329E-01

We can observe from Fig. 5 and Fig. 6 that the results of radial stresses σ_r calculated by using the CBEM become less satisfactory as the computed points locate increasingly close to the boundary, i.e., when the distance between the interior point

Table 2: Tangential stresses σ_θ at interior points close to the inner surface

Radius r	Exact	CBEM	Present	Relative error
1.1	0.7176309E+01	0.7177468E+01	0.7177468E+01	-0.1616178E-01
1.04	0.7830375E+01	0.7810632E+01	0.7833678E+01	-0.4218329E-01
1.01	0.8201974E+01	0.5963880E+01	0.8207646E+01	-0.6916232E-01
1.001	0.8320020E+01	0.1187044E+02	0.8326496E+01	-0.7783813E-01
1.0001	0.8332000E+01	0.1319104E+02	0.8338553E+01	-0.7864782E-01
1.00001	0.8333200E+01	0.1332452E+02	0.8339803E+01	-0.7923699E-01
1.000001	0.8333320E+01	0.1333787E+02	0.8339923E+01	-0.7923119E-01
1.0000001	0.8333332E+01	0.1333921E+02	0.8339887E+01	-0.7865526E-01
1.00000001	0.8333333E+01	0.1333934E+02	0.8338562E+01	-0.6274595E-01
1.000000001	0.8333333E+01	0.1333935E+02	0.8343783E+01	-0.1253925E+00
1.0000000001	0.8333333E+01	0.1333935E+02	0.8341133E+01	-0.9360174E-01

and the boundary is equal to or less than 0.05. By using the same mesh, the present method gains excellent accuracy even when the distance between the interior point and the outer boundary approaches 10^{-10}.

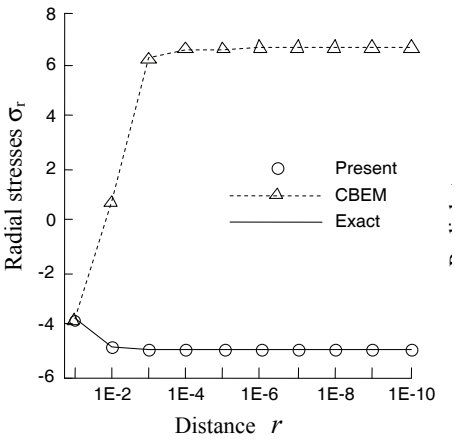

Figure 6: Radial stresses σ_r at interior points close to the inner surface

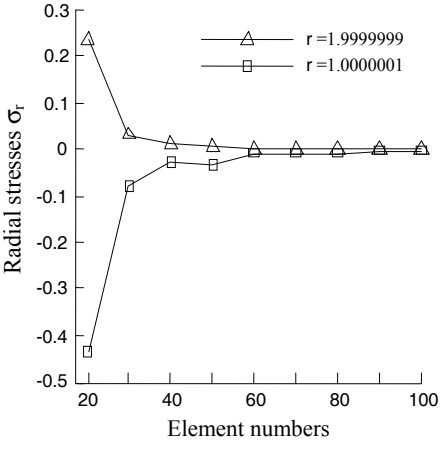

Figure 7: Convergence curves of the computed σ_θ

In addition, the convergence curves in Fig. 7 show that the convergence rates of the present method are fast even when the distance between the computed point and the boundary reaches 10^{-7}.

Example 2 As shown in Fig. 8, an infinite plate with a circular hole subjected to

the uniform tensile forces $p = 2$ at infinity is considered. The radius of the circle is $r = 1$. In this example, the elastic shear modulus G and the Poisson's ratio v are the same as in the example 1. There are 20 uniform quadratic boundary elements divided along the circular boundary.

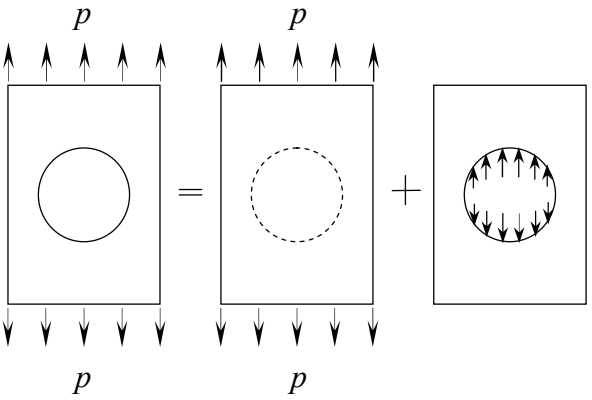

Figure 8: An infinite plate with a circular hole subjected to the uniform tensile forces

Table 3: Tangential stresses σ_θ at interior points on the line $x_2 = 0$

Coordinatex_1	Exact	CBEM	Present	Relative error
1.1	0.4875487E+01	0.4876466E+01	0.4876466E+01	-0.2009130E-01
1.01	0.5863237E+01	0.5805375E+01	0.5866426E+01	-0.5438222E-01
1.001	0.5986033E+01	0.6103824E+01	0.5989719E+01	-0.6157678E-01
1.0001	0.5998600E+01	0.6148594E+01	0.6002340E+01	-0.6234624E-01
1.00001	0.5999860E+01	0.6153027E+01	0.6003606E+01	-0.6243178E-01
1.000001	0.5999986E+01	0.6153470E+01	0.6003737E+01	-0.6251000E-01
1.0000001	0.5999999E+01	0.6153514E+01	0.6003735E+01	-0.6226901E-01
1.00000001	0.6000000E+01	0.6153518E+01	0.6003726E+01	-0.6210675E-01
1.000000001	0.6000000E+01	0.6153519E+01	0.6003862E+01	-0.6437451E-01
1.0000000001	0.6000000E+01	0.6153519E+01	0.6003715E+01	-0.6191998E-01

Tab. 3 presents the results of tangential stresses σ_θ calculated by using both the CBEM and the present method at interior points on the line $x_2 = 0$. It can be seen that the results calculated by the CBEM are not in a good agreement with the

Table 4: Tangential stresses σ_θ at interior points with the radius of $r = 1.000000001$

Angle θ	Exact	CBEM	Present	Relative error
0	0.6000000E+01	0.6153519E+01	0.6003862E+01	-0.6437451E-01
$\pi/10$	0.5236068E+01	0.5503660E+01	0.5239481E+01	-0.6518125E-01
$2\pi/10$	0.3236068E+01	0.3802308E+01	0.3238303E+01	-0.6906802E-01
$3\pi/10$	0.7639320E+00	0.1699320E+01	0.7647112E+00	-0.1019982E+00
$4\pi/10$	-0.1236068E+01	-0.2032196E-02	-0.1236467E+01	-0.3232167E-01
$5\pi/10$	-0.2000000E+01	-0.6518910E+00	-0.2000850E+01	-0.4251437E-01
$6\pi/10$	-0.1236068E+01	-0.2032196E-02	-0.1236469E+01	-0.3240459E-01
$7\pi/10$	0.7639320E+00	0.1699320E+01	0.7647094E+00	-0.1017558E+00
$8\pi/10$	0.3236068E+01	0.3802308E+01	0.3238301E+01	-0.6901786E-01
$9\pi/10$	0.5236068E+01	0.5503660E+01	0.5239480E+01	-0.6516227E-01
π	0.6000000E+01	0.6153519E+01	0.6003862E+01	-0.6437451E-01

analytic solutions as the computed points locate increasingly close to the boundary, i.e., when the distance between the interior point and the boundary is equal to or less than 0.01. However, the results calculated by the proposed method are very consistent with the exact solutions even when the distance between the interior point and the outer boundary approaches 10^{-10}. The percentage errors are also listed in Tab. 3, from which we can see that the accuracy of the results calculated by the present method are high and stable with the largest relative error less than 0.07%.

For different angles, the calculation results of tangential stresses σ_θ at interior points with radius of 1.000000001 are listed in Tab. 4, from which we can observe that the results calculated by the CBEM become less satisfactory or even invalid. In contrast with the CBEM, the present method can be applied successfully to obtain accurate results at these interior points.

The results of radial stresses σ_r at interior points on the line $x_2 = 0$ are shown in Fig. 9, from which we can see that the present method yields excellent accuracy even when the distance between the interior point and the inner surface reaches 10^{-10}. In addition, the convergence plot in Fig. 10 shows that the convergence rates of the present method are fast even when the distance between the computed point and the boundary approaches 10^{-9}.

Example 3 An infinite plate with a circular hole subjected to a uniform radial pressure $p = 5$, as shown in Fig. 11. The radius of the circle is $r = 5$. In this example, the elastic shear modulus$G$ and the Poisson's ratio v are the same as in the example 1.

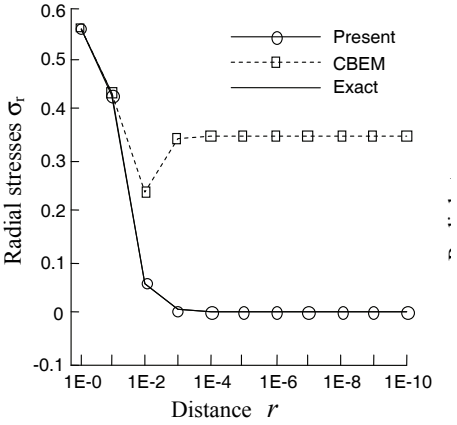

Figure 9: Radial stresses σ_r at interior points on the line $x_2 = 0$

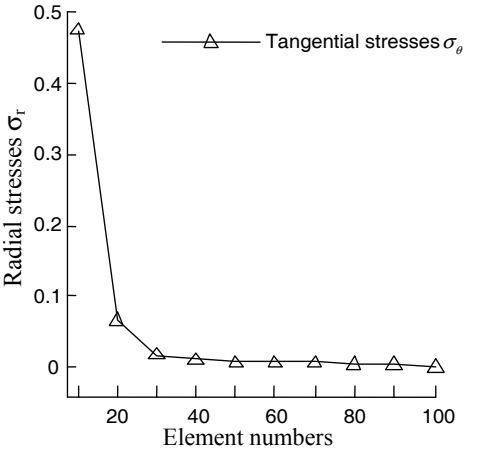

Figure 10: Convergence curve of the computed σ_θ at the point (1E-09, 0)

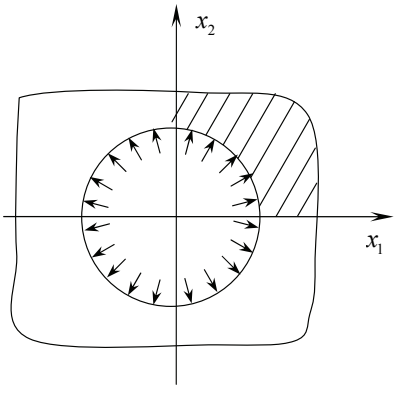

Figure 11: An infinite plate with a circular hole subjected to a uniform radial pressure

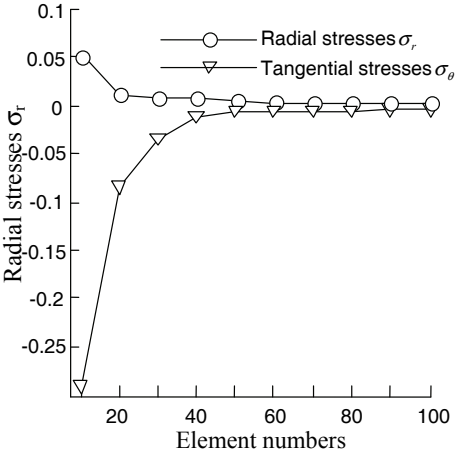

Figure 12: Convergence curves of the stresses σ_r and σ_θ at the point (5E-07, 0)

The boundary is discretized into twenty quadratic elements. For the interior points increasingly close to the boundary, the results of the radial and tangential stresses, σ_r and σ_θ, on the line $x_2 = 0$ are listed in Tab. 5 and Tab. 6, respectively. It can be observed that the values of the interior stresses obtained by using the CBEM become deviated when $x_1 < 5.2$. In contrast, the present method can obtain excellent

results with the largest relative error less than 0.06% for radial stresses and 0.2% for tangential stresses even when $x_1 = 5.0000000001$.

Table 5: Radial stresses σ_r at interior points on the line $x_2 = 0$

Radius r	Exact	CBEM	Present	Relative error
5.2	-0.462278E+01	-0.4590583E+01	-0.4621969E+01	0.1757317E-01
5.1	-0.480584E+01	-0.3778935E+01	-0.4805366E+01	0.9943386E-02
5.01	-0.498006E+01	0.3201157E+01	-0.4980010E+01	0.9963969E-03
5.001	-0.499800E+01	0.3696937E+01	-0.4997996E+01	0.9480385E-04
5.0001	-0.499980E+01	0.3743547E+01	-0.4999791E+01	0.1804154E-03
5.00001	-0.499998E+01	0.3748205E+01	-0.5000032E+01	0.1049353E-02
5.000001	-0.499999E+01	0.3748671E+01	-0.4999921E+01	0.1531263E-02
5.0000001	-0.500000E+01	0.3748718E+01	-0.4999513E+01	0.9744626E-02
5.00000001	-0.500000E+01	0.3748722E+01	-0.5000367E+01	0.7330816E-02
5.000000001	-0.500000E+01	0.3748723E+01	-0.5002389E+01	0.4778081E-01
5.0000000001	-0.500000E+01	0.3748723E+01	-0.5002995E+01	0.5990278E-01

Table 6: Tangential stresses σ_θ at interior points on the line $x_2 = 0$

Radius r	Exact	CBEM	Present	Relative error
5.2	0.4622781E+01	0.4600389E+01	0.4624871E+01	-0.4521102E-01
5.1	0.4805844E+01	0.4163711E+01	0.4809111E+01	-0.6798521E-01
5.01	0.4980060E+01	0.6704914E+01	0.4984544E+01	-0.9004280E-01
5.001	0.4998001E+01	0.8542143E+01	0.5002605E+01	-0.9213396E-01
5.0001	0.4999800E+01	0.8732868E+01	0.5004408E+01	-0.9217102E-01
5.00001	0.4999980E+01	0.8751950E+01	0.5004650E+01	-0.9339370E-01
5.000001	0.4999998E+01	0.8753859E+01	0.5004510E+01	-0.9023574E-01
5.0000001	0.5000000E+01	0.8754049E+01	0.5004211E+01	-0.8422029E-01
5.00000001	0.5000000E+01	0.8754068E+01	0.5005206E+01	-0.1041124E+00
5.000000001	0.5000000E+01	0.8754070E+01	0.5006909E+01	-0.1381724E+00
5.0000000001	0.5000000E+01	0.8754071E+01	0.5006582E+01	-0.1316304E+00

In addition, the convergence rates of the radial and tangential stresses, σ_r and σ_θ, at the point $(5.0000001, 0)$ are shown in Fig. 12, from which we can observe that the convergence rates of the computed stresses σ_r and σ_θ are acceptable even when the distance between the computed point and the boundary reaches 10^{-7}.

6 Conclusions

In the present paper, a general strategy based on a nonlinear transformation is proposed in order to calculate the nearly singular integrals occurring on high-order geometrical elements. The strategy produces very high accuracy for determining the nearly singular integrals even when the distance between the field points and the integral elements are as small as $1.0\mathrm{E}-9$. Three numerical examples show that the present algorithm has been successfully employed in the numerical calculation of nearly singular integrals on curved elements. As a result, accurate stress results of the interior points close to the boundary are achieved. The present method is also general and can be applied to other problems in BEM (such as thin-walled structures), which will be discussed later.

Acknowledgement: The research is supported by the National Natural Science Foundation of China (no. 10571110) and the Natural Science Foundation of Shandong Province of China (no. 2003ZX12).

References

Albuquerque, E.L.; Aliabadi, M.H. (2008): A Boundary Element Formulation for Boundary Only Analysis of Thin Shallow Shells. *CMES: Computer Modeling in Engineering and Sciences*, vol. 29, no. 2, pp. 63-73.

Atluri, S.N. (2004a): *The meshless method (MLPG) for domain and BIE discretizations*. Forsyth, GA, USA, Tech Science Press.

Atluri, S.N. (2005): *Methods of computer modeling in engineering and the sciences*. Tech Science Press.

Atluri, S.N.; Han, Z.D.; Rajendran, A.M. (2004b): A new implementation of the meshless finite volume method through the MLPG "mixed" approach. *CMES: Computer Modeling in Engineering and Sciences*, vol. 6, no. 6, pp. 491-514.

Atluri, S.N.; Liu, H.T.; Han, Z.D. (2006): Meshless local Petrov-Galerkin (MLPG) mixed collocation method for elasticity problems. *CMES: Computer Modeling in Engineering and Sciences*, vol. 14, no. 3, pp. 141-152.

Brebbia, C.A.; Tells, J.C.F.; Wrobel, L.C. (1984): *Boundary Element Techniques*. Berlin, Heidelberg, New York, Tokyo: Springer.

Cerrolaza, M.; Alarcon, E. (1989): A bi-cubic transformation of the Cauchy principal value integrals in boundary methods. *Int J Numer Methods Engng*, vol. 28, pp. 987-999.

Chen, H.B.; Lu, P.; Huang, M.G.; Williams, F.W. (1998): An effective method for finding values on and near boundaries in the elastic BEM. *Comput Struct*, vol.

69(4), pp. 421-431.

Chen, J.T. (2000): Recent development of dual BEM in acoustic problems. *Comput Methods Appl Mech Eng*, vol. 188, pp. 833-845.

Chen, J.T.; Chen, K.H.; Chen, C.T. (2002): Adaptive boundary element method of time-harmonic exterior acoustics in two dimensions. *Comput Methods Appl Mech Eng*, vol. 191, pp. 3331–3345.

Chen, X.L.; Liu, Y.J. (2001): Thermal stress analysis of multi-layer thin films and coatings by an advanced boundary element method. *CMES: Computer Modeling in Engineering and Sciences*, vol. 2(3), pp. 337– 49.

Cruse, T.A. (1974): An improved boundary integral equation method for three dimensional elastic stress analysis. *Compt Struct*, vol. 4, pp. 741-754.

Cruse, T.A.; Aithal, R.A. (1993): A new integration algorithm for nearly singular BIE kernels. *Int J Numer Methods Eng*, vol. 36, pp. 237-254.

Davies, A.J.; Crann, D.; Kane, S.J.; Lai, C.H. (2007): A Hybrid Laplace Transform/Finite Difference Boundary ElementMethod for Diffusion Problems. *CMES: Computer Modeling in Engineering and Sciences*, vol. 18, no. 2, pp. 79-85.

Earlin, L. (1992): Exact Gaussian quadrature methods for near-singular integrals in the boundary element method. *Eng Anal Bound Elem*, vol. 9, pp. 233-245.

Earlin, L. (1993): A mapping method for numerical evaluation of two-dimensional integrals with singularity. *Compul Mech*, vol. 12, pp. 19- 26.

Fratantonio, M.; Rencis, J.J. (2000): Exact boundary element integrations for two-dimensional Laplace equation. *Eng Anal Bound Elem*, vol. 24, pp. 325–42.

Friedrich, F. (2002): A linear analytical boundary element method for 2D homogeneous potential problems. *Comput Geosci*, vol. 28, pp. 679–92.

Gao, X.W.; Yang, K.; Wang, J. (2008): An adaptive element subdivision technique for evaluation of various 2D singular boundary integrals. *Eng Anal Bound Elem*, vol. 32, pp. 692–696.

Gray, L.J.; Garzon, M.; Mantic, V.E. (2006): Graciani, Galerkin boundary integral analysis for the axisymmetric Laplace equation. *Int J Numer Methods Eng*, vol. 66, pp. 2014–2034.

Granados, J.J.; Gallego, G. (2001): Regularization of nearly hypersingular integrals in the boundary element method. *Eng Anal Bound Elem*, vol. 25, pp. 165-184.

Guiggiani, M.; Krishnasamy, G.; Rudolphi, T.J.; Rizzo, F.J. (1992): A general algorithm for the numerical solution of hypersingular BEM. *J Appl Mech*, vol. 59, pp. 604- 627.

Guz, A.N.; Menshykov, O.V.; Zozulya, V.V.; Guz, I.A. (2007): Contact Problem for the Flat Elliptical Crack under Normally Incident ShearWave. *CMES: Computer Modeling in Engineering and Sciences*, vol. 17, no. 3, pp. 205-214.

Huang, Q.; Cruse, T.A. (1993): Some notes on singular integral techniques in boundary element analysis. *Int J Numer Methods Engng*, vol. 36, pp. 2643-2659.

Johnston, P.R. (1999): Application of sigmoidal transformations to weakly singular and near singular boundary element integrals. *Int J Numer Meth Eng*, vol. 45, pp. 1333-1348.

Johnston, P.R. (2000): Semi-sigmoidal transformations for evaluating weakly singular boundary element integrals. *Int J Numer Meth Eng*, vol. 47, pp. 1709-1730.

Jun, L.; Beer, G.; Meek (1985): Efficient evaluation of integrals of order using Gauss quadrature. *Engng Anal*, vol. 2, pp. 118-23.

Karlis, G.F.; Tsinopoulos, S.V.; Polyzos, D.; Beskos, D.E. (2008): 2D and 3D Boundary Element nalysis of Mode-I Cracks in Gradient Elasticity. *CMES: Computer Modeling in Engineering and Sciences*, vol. 26, no. 3, pp. 189-207.

Lachat, J.C.; Watson, J.O. (1976): Effective numerical treatment of boundary integral equation: a formulation for elastostatics. *Int J Numer Meth Eng*, vol. 21, pp. 211-228.

Li, J.; Wu, J.M.; Yu, D.H. (2009): Generalized Extrapolation for Computation of Hypersingular Integrals in Boundary Element Methods. *CMES: Computer Modeling in Engineering and Sciences*, vol. 42, no. 2, pp. 151-175.

Lifeng, M.A.; Alexander, M.; Korsunsky (2004): A note on the Gauss-Jacobi quadrature formulae for singular integral equations of the second kind. *Int J Fract*, vol. 126, pp. 339-405.

Liu, C.S.; Chang, C.W.; Chang, J.R. (2008): A New Shooting Method for Solving Boundary Layer Equations in Fluid Mechanics. *CMES: Computer Modeling in Engineering and Sciences*, vol. 32, no. 1, pp. 1-15.

Liu, Y.J. (1998): Analysis of shell-like structures by the boundary element method based on 3-D elasticity: formulation and verification. *Int J Numer Meth Engng*, vol. 41, pp. 541-558.

Luo, J.F.; Liu, Y.J.; Berger, E.J. (1998): Analysis of two- dimensional thin structures (from micro- to nano-scales) using the boundary element method. *Comput Mech*, vol.22, pp. 404-412.

Ma, H.; Kamiya, N. (2002): Distance transformation for the numerical evaluation of near singular boundary integrals with various kernels in boundary element method. *Eng Anal Bound Elem*, vol.26, pp. 329- 339.

Mukherjee, S.; Chati, M.K.; Shi, X.L. (2000): Evaluation of nearly singular inte-

grals in boundary element contour and node methods for three-dimensional linear elasticity. *Int J Sol Struct*, vol. 37, pp. 7633-7654.

Niu, Z.R.; Cheng, C.Z.; Zhou, H.L.; Hu, Z.J. (2007): Analytic formulations for calculating nearly singular integrals in two-dimensional BEM. *Eng Anal Bound Elem*, vol. 31, pp. 949–964.

Sanz, J.A.; Solis, M.; Domingnez, J. (2007): Hypersingular BEM for Piezoelectric Solids: Formulation and Applications for FractureMechanics. *CMES: Computer Modeling in Engineering and Sciences*, vol. 17, no. 3, pp. 215-229.

Sladek, V.; Sladek, J.; Tanaka, M. (1993): Regularization of hypersingular and nearly singular integrals in the potential theory and elasticity. *Int J Numer Methods Eng*, vol. 36, pp. 16-28.

Sladek, V.; Sladek, J.; Tanaka, M. (2000): Optimal transformations of the integration variables in computation of singular integrals in BEM. *Int J Numer Methods Eng*, vol. 47, pp. 1263-1283.

Sun, H.C.; Zhang, L.Z.; Xu, Q.; Zhang, Y.M. (1999): *Nonsingular Boundary Element Method*. *Dalian*: Dalian University of Technology Press (in Chinese).

Tanaka, M.; Matsumoto, T.; Nakamura, M. (1991): *Boundary element method*. Baifukan Press, Tokyo (in Japanese).

Tanaka, M.; Sladek, V.; Sladek, J. (1994): Regularization techniques applied to BEM. *Appl Mech Rev*, vol. 47, pp. 457–499.

Telles, J.C.F. (1987): A self-adaptive coordinate transformation for efficient numerical evaluation of general boundary element integral. *Int J Numer Meth Eng*, vol. 24, pp. 959-973.

Wang, Y.C.; Li, H.Q.; Cheng, H.B.; Wu, Y. (1994) Calculating the stresses and displacements at arbitrary points with the particular solution field method. *Acta Mech Sin*, vol. 26(2), pp. 222-231.

Yoon, S.S.; Heister, S.D. (2000): Analytic solution for fluxes at interior points for 2D Laplace equation. *Eng Anal Bound Elem*, vol. 24, pp. 155–60.

Young, D.L.; Chen, K.H.; Chen, J.T.; Kao, J.H. (2007): A Modified Method of Fundamental Solutions with Source on the Boundary for Solving Laplace Equations with Circular and Arbitrary Domains. *CMES: Computer Modeling in Engineering and Sciences*, vol. 19, no. 3, pp. 197-221.

Zhang, Y.M.; Wen, W.D. (2004): A kind of new nonsingular boundary integral equations for elastic plane problems. *Acta Mech,* vol.36(3), pp. 311-321 (in Chinese).

Zhang, Y.M.; Sun, C.L. (2008): A general algorithm for the numerical evaluation of nearly singular boundary integrals in the equivalent non-singular BIES with

indirect unknowns. *Journal of the Chinese Institute of Engineers*, vol. 31, pp. 437-447.

Zhang, Y.M.; Sun, H.C. (2001): Analytical treatment of boundary integrals in direct boundary element analysis of plane potential and elasticity problems. *Appl Math Mech*, vol. 6, pp. 664-673.

Zhang, Y.M.; Sun, H.C. (2000): Theoretic Analysis on Virtual Boundary Element. *Chinese J Comp Mech*, vol.17, pp. 56-62 (in Chinese).

Zhang, X.S.; Zhang, X.X. (2004): Exact integrations of two-dimensional high-order discontinuous boundary element ofelastostatics problems. *Eng Anal Bound Elem*, vol. 28, pp. 725-732.

Zhou, H. L.; Niu, Z. R.; Cheng, C. Z. (2008): Analytical integral algorithm applied to boundary layer effect and thin body effect in BEM for anisotropic potential problems. *Comp and Struct*, vol.86, pp. 1656– 1671.